Journal of Nuclear Materials 412 (2011) 123–128

Contents lists available at ScienceDirect

Journal of Nuclear Materials

journal homepage: www.elsevier.com/locate/jnucmat

Theoretical studies of macroscopic erosion mechanisms of melt layers developed on plasma facing components

Y. Shi *, G. Miloshevsky, A. Hassanein

School of Nuclear Engineering, Center for Materials Under Extreme Environment, Purdue University, West Lafayette, IN 47907, USA

ARTICLE INFO

Article history:
Received 29 September 2010
Accepted 17 February 2011
Available online 5 March 2011

ABSTRACT

During plasma instabilities in tokamak devices, metallic plasma facing components (PFC) undergo surface vaporization and melting. Macroscopic losses of melt layers are of a serious concern to the lifetime of PFC, the damage of nearby components, and potential core plasma contamination. A normal or inclined plasma stream flowing at the melt layer surface of PFC at very high velocities ($\sim 10^5$ m/s) can induce Kelvin–Helmholtz (K–H) instabilities. We present an extensive linear stability theory and capillary droplet ejection model adapted to the problem of melt layer erosion and splashing. Based on this linear analysis, the stability criterion is established accounting the influence of the thicknesses of both plasma stream and melt layer. The growth rate of the most unstable wave is investigated with respect to different parameters such as plasma density and velocity, material properties, and melt layer thickness. A capillary droplet ejection model is then developed and used to analytically estimate the erosion rate of the melt layer for tungsten and aluminum targets. The present work brings a detailed understanding of the onset of K–H instabilities developed in melt layers due to plasma stream impact and builds a theoretical basis to estimate a macroscopic erosion rate, material losses and lifetime for PFC.

Published by Elsevier B.V.

1. Introduction

In a tokamak chamber, during normal or off-normal operating conditions, plasma facing components (PFC) are subjected to high-energy depositions ($\sim$10 to $\sim$100 GW/m^2 during 0.1–1 ms) as a result of plasma instabilities such as disruptions, giant edge-localized modes (ELM), and vertical displacement events [1]. The immediate consequence is vaporization and melting of PFC. Although the vapor-shielding phenomenon, i.e., accumulation of the materials own vapor in front of the incoming plasma stream, considerably reduces material losses from the surface [2], the continued plasma-target interaction can cause consequent damage to PFC due to macroscopic erosion of the developed melt layer, whose thickness is much larger than the net surface vaporization and can range from tens to hundreds of microns per one event of plasma instabilities [3].

The melt layer erosion of tungsten and aluminum has been investigated both theoretically [4,5] and experimentally [6,7]. The experimental observations show the ejection of liquid metal droplets during heating of the target. Different phenomena like intense boiling and hydrodynamic instabilities are identified as the main erosion mechanisms. The models implemented in the current computer codes [8,9] provide an estimate of the erosion rate of the metallic targets. A more detailed physical understanding of the erosion mechanisms is required to improve the computational modeling and provide realistic lifetime estimates of PFC.

As discussed in [10,11], the interaction between the plasma stream and the melt layer is seen as a parallel two-fluid flow. In the inviscid model, due to the high velocity difference, Kelvin–Helmholtz (K–H) instabilities arise from small interfacial perturbations. The early exponential growth stage of the waves was well characterized using the linear theory described in detail by Chandrasekhar [12] or Drazin and Reid [13]. Since perturbations with a wide range of wavelengths are present at the surface of the melt layer, the behavior of the most unstable wave should provide a good estimate of the arising K–H instability characteristics. The late behavior of the most unstable wave is characterized by the ejection of capillary droplets. This theory was first presented for the case of laser-pulse induced melt droplet ejection [14], where the K–H instabilities are generated by the high dynamic pressure $\rho_p V_p^2$ ($\sim$45 MPa) of ablated vapor flux at the target surface, where ρ_p and V_p are respectively the density and the velocity of the plasma. Later the theory of capillary droplets escape due to K–H instabilities was used to describe the interaction of plasma stream ($\sim$1 MPa) with tungsten melt layer [5]. However, at lower plasma dynamic pressure ($\sim$0.01 MPa), the computational fluid dynamics (CFD) simulations [10,11] show the growth of continuous liquid tungsten ligaments for a certain range of perturbation wavelengths, which eventually breaks into droplets. Dedicated melt experiments carried out in the tokamak TEXTOR device also

* Corresponding author. Address: Potter Building (Purdue University), 400 Central Drive, West Lafayette, IN 47907-2063, USA. Tel.: +1 33 6 99 87 00 94.
E-mail addresses: shi24@purdue.edu, yimeng.shi@mines.nancy-inpl.fr (Y. Shi).

0022-3115/$ - see front matter Published by Elsevier B.V.
doi:10.1016/j.jnucmat.2011.02.041

demonstrate the loss of molten tungsten in the form of continuous fine spray with droplets [15]. Therefore, the formation of single droplets or continuous droplet-like ligaments, depending on parameters such as the plasma dynamic pressure, should be investigated in more details.

In the present work, a comprehensive linear stability theory is presented and a detailed analysis of K–H instabilities, in the frame of plasma and melt-layer interaction, is performed. First, the stability criterion, the cut-off wavelengths, etc., are investigated. Then, the behavior of the most unstable wave is studied in the linear stage and extended to the non-linear stage using the above quoted capillary droplet theory. Finally, a one-dimensional erosion rate due to K–H splashing is derived. Overall, the influence of different parameters such as the thicknesses of the plasma stream and the melt layer, the plasma density and the materials properties (density and surface tension) is studied and discussed. Furthermore, the implication of melt layer splashing and loss on the PFC lifetime is briefly discussed.

2. Theory

We assume that the perturbation normal to the melt layer surface has the shape of the following complex wave function [13]:

$$\hat{\xi}(\tau,x)=\xi_0\exp(i(\omega\tau+kx)) \tag{1}$$

where ξ_0 is the amplitude of incipient surface perturbations, ω is the angular frequency, k is the wave number, which is related to the wavelength λ by $k\lambda=2\pi$, τ and x are the time and space variables respectively. The temporal growth of the perturbations is studied in the present work, which means k is assumed real and ω can be complex. A well-established form of the dispersion relation for the linear analysis of K–H instabilities with the assumption of an inviscid and incompressible flow [12] was used in the recent study [10]. The equation was then adapted to the case where both the melt layer and the plasma stream have nearly the same or equal finite thickness [10,11]. This case of practical interest was dictated to finite dimensions of the computational domain, where a plasma height significantly larger than the melt layer thickness cannot be easily modeled.

In the present paper, we consider a more general form of the dispersion relation with different thicknesses of the melt layer and the plasma stream. The general dispersion relation can be written as [16]

$$\omega=-k\frac{\rho_p\coth(kh_p)V_p+\rho_m\coth(kh_m)V_m}{\rho_p\coth(kh_p)+\rho_m\coth(kh_m)}\pm\sqrt{\frac{\sigma k^3+gk(\rho_m-\rho_p)}{\rho_p\coth(kh_p)+\rho_m\coth(kh_m)}-\frac{\rho_p\coth(kh_p)\rho_m\coth(kh_m)k^2(V_p-V_m)^2}{(\rho_p\coth(kh_p)+\rho_m\coth(kh_m))^2}} \tag{2}$$

where the fluid subscripts m and p refer to the melt layer and the plasma stream respectively; g is the gravity acceleration; ρ, V, and h are respectively the fluid density, velocity, and the fluid layer thickness and σ is the surface tension of the liquid metal. In Eq. (2), the first term is the phase shift of the perturbation with respect to time. The expression under the square root is defined here as the stability function $\Omega(k)$. If $\Omega(k)$ is positive, the perturbation described by Eq. (1) is stable oscillating with respect to both time and space. Otherwise, the square root is a pure imaginary number and the amplitude of the perturbation has a diverging exponential time-dependence (unstable). The first term of $\Omega(k)$ is surface tension and gravity stabilizing forces. The second and negative term is the inertia term, which contributes to the growth of the instabilities and depends on the relative velocity.

Since liquid metal is usually 8–10 orders of magnitude denser than plasma vapor, we have $\rho_m\gg\rho_p$. Besides, the plasma stream thickness is usually large compared to the melt layer thickness meaning that $\coth(kh_p)$ is always smaller than $\coth(kh_m)$ for the same value of k. It is, therefore, possible to make the following assumption for any wave number:

$$\rho_p\coth(kh_p)+\rho_m\coth(kh_m)\approx\rho_m\coth(kh_m) \tag{3}$$

Then Eq. (2) is simplified to

$$\omega=-k\left(V_m+\frac{\rho_p\tanh(kh_m)}{\rho_m\tanh(kh_p)}V_p\right)\pm\sqrt{\left(\frac{\sigma}{\rho_m}k^3+gk\right)\tanh(kh_m)-\frac{\rho_p\tanh(kh_m)}{\rho_m\tanh(kh_p)}k^2\Delta V^2} \tag{4}$$

By taking $h_m=h_p$, Eq. (4) becomes the expression provided in [10]. The stability function defined previously is then given by:

$$\Omega(k)=\left(\frac{\sigma}{\rho_m}k^3+gk\right)\tanh(kh_m)-\frac{\rho_p\tanh(kh_m)}{\rho_m\tanh(kh_p)}k^2\Delta V^2 \tag{5}$$

In our problem, the melt layer thickness is on the order of ~10 to ~400 μm, whereas the plasma stream can be considered as infinitely thick. Therefore, the stability function can be simplified to:

$$\Omega(k)=\left[\left(\frac{\sigma}{\rho_m}k^3+gk\right)-\frac{\rho_p}{\rho_m}k^2\Delta V^2\right]\tanh(kh_m) \tag{6}$$

The system becomes unstable for $\Omega(k)<0$, which provides the following stability criterion derived from Eq. (5)

$$|\Delta V|^2>\left(\frac{g\rho_m}{k}+\sigma k\right)\frac{\tanh(kh_p)}{\rho_p} \tag{7}$$

We now derive the critical wave number and velocity difference using Eq. (7). At large wavelengths, Eq. (7) shows that gravity controls the critical velocity and stabilizes the perturbations, and at small wavelengths, the surface tension is the stabilizing factor. It is worth noting, due to the large density difference between the plasma and the liquid metal, the critical velocity difference depends on the thickness of the plasma stream only and not on the thickness of the melt layer. Using the assumption of infinitely thick plasma layer, $\tanh(kh_p)\to1$, and the stability criterion of Eq. (7), simple expressions for the critical wavelength and the critical relative velocity are derived by finding the minimum with respect to the wave number of the RHS of Eq. (7)

$$k_c=\sqrt{\frac{g\rho_m}{\sigma}}\Longleftrightarrow\lambda_c=2\pi\sqrt{\frac{\sigma}{g\rho_m}} \tag{8}$$

Substituting k_c into Eq. (7) we can get the critical velocity

$$\Delta V_c^2=\left(\frac{g\rho_m}{k_c}+\sigma k_c\right)\frac{\tanh(k_ch_p)}{\rho_p}=\frac{2}{\rho_p}\sqrt{\sigma g\rho_m} \tag{9}$$

The critical wavelength is commonly known as the Taylor wavelength. It represents the first wave to become unstable with increasing relative velocity. For a relative velocity lower than the critical one, perturbations with any wavelength are stable. For relative velocity larger than the critical value, only wavelengths of a certain range are unstable.

The range of unstable waves can be derived using Eq. (6). It is delimited by the following cut-off wave numbers found by equaling $\Omega(k)$ to zero in Eq. (6) and solving the quadratic equation

$$k_{1,2}=\frac{\rho_p\Delta V^2}{2\sigma}\left(1\pm\sqrt{1-\frac{4\sigma g\rho_m}{\rho_p^2\Delta V^4}}\right) \tag{10}$$

In this range of unstable waves for which $\Omega(k)$ is negative, $\Omega(k)$ reaches a local maximum absolute value at k_M (or λ_M), which

defines the most unstable wave. The wave number k_M represents the fastest growing perturbation for a fixed value of a relative velocity. Therefore, the local minimum of $\Omega(k)$ in Eq. (6) at k_M provides the maximum temporal increment coefficient defined as:

$$\Gamma_M = \sqrt{-\Omega(k_M)} = \left[\frac{\sigma}{\rho_m}k_M^3 - \frac{\rho_p}{\rho_m}k_M^2\Delta V^2\right]\sqrt{\tanh(k_M h_m)} \tag{11}$$

The gravity contribution is neglected because in our problem, the most unstable wavelength is relatively short, which implies the gravity effect is less significant. The most unstable wavelength and the maximum increment coefficient can be used to assess whether K–H instabilities are likely to arise for given reactor conditions and material properties. Also, since this is the wave with the fastest growth, it could be the main factor of erosion and droplets ejection. The analytic expression for the minimum of Eq. (11) cannot be derived for an arbitrary value of k. The resulting algebraic equation can only be solved numerically. However, the analytical formula can be obtained in the limiting cases of a deep and shallow melt layer with $kh_m \gg 1$ and $kh_m \ll 1$, respectively. Differentiating Eq. (6) with respect to the wave number, while neglecting the gravity term yields the following asymptotic solutions:

$$kh_m \ll 1 \Rightarrow k_M \cong \tfrac{3\rho_p\Delta V^2}{4\sigma} \quad \lambda_M \cong \tfrac{8\pi\sigma}{3\rho_p\Delta V^2} \tag{12}$$

$$kh_m \gg 1 \Rightarrow k_M \cong \tfrac{2\rho_p\Delta V^2}{3\sigma} \quad \lambda_M \cong \tfrac{3\pi\sigma}{\rho_p\Delta V^2} \tag{13}$$

The maximum increment coefficients from Eq. (11) are then

$$kh_m \ll 1 \Rightarrow \Gamma_M = \frac{3\sqrt{3}}{16}\frac{\rho_p^2\Delta V^4}{\rho_m^{\frac{1}{2}}\sigma^{\frac{3}{2}}}\sqrt{h_m} \tag{14}$$

$$kh_m \gg 1 \Rightarrow \Gamma_M = \frac{2}{3\sqrt{3}}\frac{\rho_p^{\frac{3}{2}}\Delta V^3}{\rho_m^{\frac{1}{2}}\sigma} \tag{15}$$

While the Taylor critical wave k_c of Eq. (8) depends only on the properties of the fluids, the cut-off waves $k_{1,2}$ and the most unstable wave k_M are found for a fixed relative velocity ΔV.

The real part of wave function of the most dangerous wavelength in the linear stage is obtained from the complex function of Eq. (1)

$$\begin{aligned}\xi(\tau,x) &= \Re\left[\hat{\xi}(\tau,x)\right] \\ &= \xi_0\exp(\Gamma_M\tau) \\ &\quad\times\cos\left\{\frac{2\pi}{\lambda_M}\left[x-\left(V_m+\frac{\rho_p}{\rho_m}\tanh(k_M h_m)V_p\right)\tau\right]\right\}\end{aligned} \tag{16}$$

Controlled by the maximum increment coefficient, its amplitude grows exponentially with respect to time. The growth of the instability amplitude is given by

$$U_M(\tau) = \xi_0\Gamma_M\exp(\Gamma_M\tau) \tag{17}$$

The solution of Eq. (16) is only valid in the early growth stage of the unstable wave and cannot explain the growth of the ligaments observed in the CFD simulations [10]. However, with higher momentum of the incident plasma stream due to higher plasma density ($\sim 10^{-5}$ to $\sim 10^{-4}$ kg/m^3), λ_M is expected to be shorter and Γ_M significantly larger to allow a fast growth of the surface perturbation. The capillary effect may then lead to the formation of droplets as mentioned in [4,5] with a radius approximated by $r_d = \lambda_M/4$.

The expression of the characteristic time needed for a droplet to escape from the melt surface was derived in [5] from a condition that the kinetic energy of the growing droplet equals to the energy needed to form the droplet surface:

$$\tau_{KH} = \frac{1}{\Gamma_M}\ln\left[\frac{1}{\Gamma_M\xi_0}\sqrt{\frac{24\sigma}{\lambda_M\rho_m}}\right] \tag{18}$$

The droplet escape is possible when τ_{KH} is lower than the characteristic time of plasma-target interaction. Assuming this condition is fulfilled and the target surface is covered with $1/\lambda_M^2$ droplet ejection sites per unit area, the one-dimensional erosion rate of the melt layer due to K–H instabilities can be derived as:

$$W_{KH} = \frac{1}{\tau_{KH}\lambda_M^2}\left(\frac{4}{3}\pi r_d^3\right) = \frac{\pi\lambda_M}{48\tau_{KH}} \tag{19}$$

The erosion rate in Eq. (19) is similar to the splashing wave model used in [4].

The present study only considers the interaction between plasma and melt layer as a pure hydrodynamic problem, therefore, plasma is characterized using its mass density ρ_P. However, the electron density N_e, which is more commonly used parameter to characterize plasma, can also be estimated and used in the results to improve understanding. Using the Hartree–Fock–Slater model [17,18], the ionization balance of the plasma can be calculated as a function of plasma temperature T_e. Fig. 1 shows the ionization balance for hydrogen plasma, which is used in tokamak devices such as TEXTOR [19]. In the same experimental conditions, the hydrogen plasma is characterized with a temperature of ~70 eV. For hydrogen, $N_e = N_i$, where N_i is the ion density of the plasma. Fig. 1 also shows, at ~70 eV, the hydrogen atoms are fully stripped, which makes the following approximation possible

$$N_e = N_i \approx \rho_p N_A/M_H \tag{20}$$

where N_A is the Avogadro number and M_H is the standard atomic mass of hydrogen.

3. Results and discussions

The linear stability theory of liquid metal splashing discussed above was applied to investigate the critical wavelength, growth rate of K–H instabilities, and droplets ejection from the melted surface of tungsten and aluminum targets.

Table 1 shows the values of the parameters of tungsten used in the CFD simulations in [10]. A finite plasma thickness is used only in Figs. 2 and 3. If not specified, the value of any parameter is set by default with the value from Table 1. Using the parameters from Table 1, the stability criterion of Eq. (7) is plotted in Fig. 2 for tungsten melt as a function of the wavelength for different values of plasma stream thickness. The Taylor wavelength λ_c and the critical

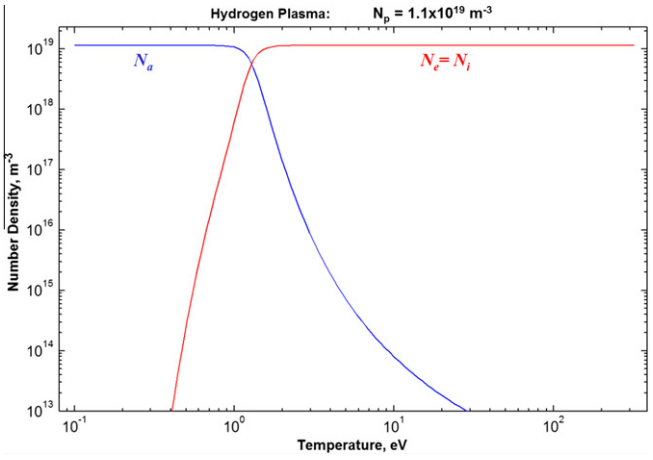

Fig. 1. The number density of atoms, ions and electrons in the hydrogen plasma as a function of the temperature for a particular plasma density 10^{-19} m^{-3}.

Table 1
Typical values of parameters used in the analysis.

g (m/s^2)	σ (N/m)	ΔV (m/s)	h_p (μm)	h_m (μm)
9.81	2.5	10^5	1600	400
N_A (mol^{-1})	M_H (kg/mol^{-1})	ρ_p (kg/m^3)	N_e (m^{-3})	ρ_m (kg/m^3)
6.022×10^{23}	1.008×10^{-3}	10^{-6}	6×10^{20}	1.76×10^4

relative velocity ΔV_c are dashed for the case of an infinitely thick plasma stream. The region of the K–H instability numerically observed in the CFD simulations [10] corresponds to the maximum velocity 10^5 m/s and the cut-off wavelength ~2.2 mm. The thickness of the plasma does not affect the stability of short waves. The stability of long waves is independent of the wavelength and increases as a function of the plasma stream thickness. The plateau at large wavelengths is given by the limit of the RHS of Eq. (7) as $\sqrt{g(\rho_m/\rho_p)h_p}$. In general the stability criterion depends on the density of fluids, the surface tension, and the body force (Eqs. (6) and (9)).

In Fig. 3, the stability function of Eq. (6) (infinitely thick plasma stream) is plotted for different values of the melt layer thickness (solid lines). While the range of the unstable waves remains the same, the most unstable wave number is weakly dependent on the melt thickness shifting slightly towards larger wave numbers. The temporal increment of the most unstable wave increases with melt layer thickness and reaches the maximum value given by Eq. (11). Fig. 3 also shows the stability function of Eq. (5) considering a finitely thick plasma stream. The values of the parameters are all taken from Table 1. The most unstable wave has a wave number $k_M = 2840$ m^{-1}, which corresponds to a wavelength of ~2.2 mm. This value is consistent with the one reported in the CFD simulations [10]. The overlapping of the dashed curve with the solid curve for a tungsten melt layer thickness of 400 μm also shows that, the 1600-μm plasma thickness used in [10] can be considered as an infinite plasma layer with very high accuracy.

From Figs. 4–8 , the electron density of the plasma N_e is estimated with Eq. (20). It is assumed that the temperature of the hydrogen plasma under tokamak conditions is higher than ~2 eV and $N_e = N_i$ (Fig. 1). Fig. 4 shows the maximum increment coefficient (Eq. (11)) as a function of the tungsten melt layer thickness for different values of plasma density. The most unstable wavelength and its temporal increment coefficient are very sensitive to several parameters such as the plasma density, which increases the increment coefficient and shorten the most unstable

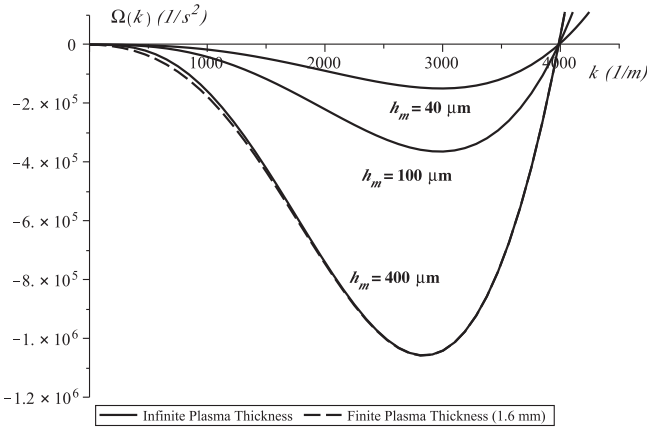

Fig. 3. Stability function for different fluid thicknesses.

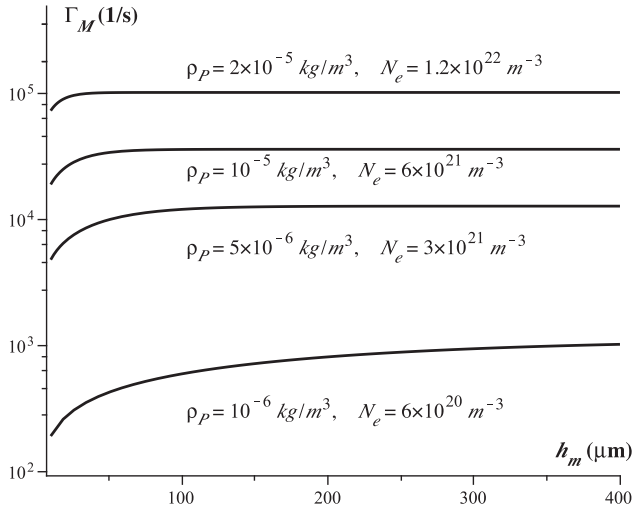

Fig. 4. Maximum increment coefficient versus melt layer thickness for different values of plasma density.

wavelengths and the surface tension, which increases the wavelength and reduces the maximum increment (Eqs. (12)–(15)). The exponent ½ of the melt layer density in Eqs. (14) and (15) shows

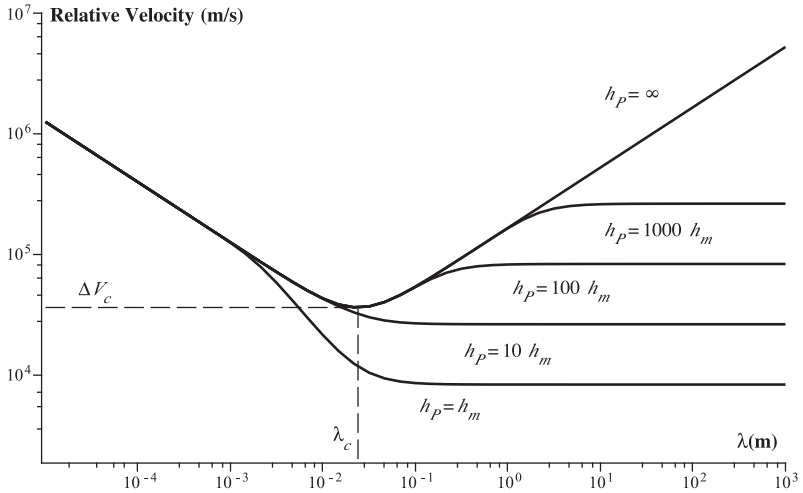

Fig. 2. Stability criterion for different plasma stream thicknesses.

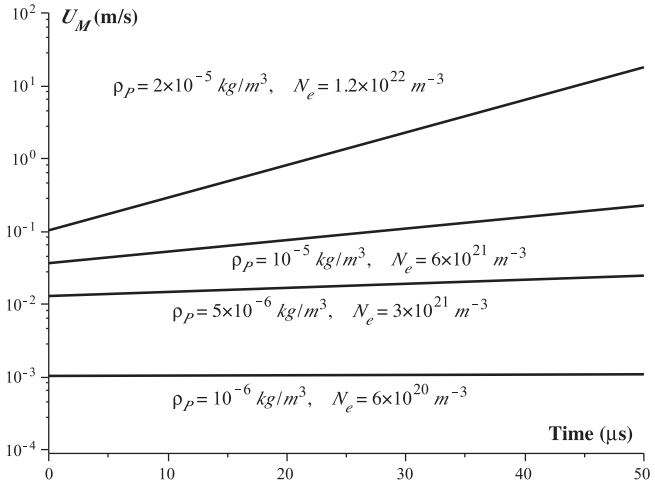

Fig. 5. Instability growth rate for different values of plasma density.

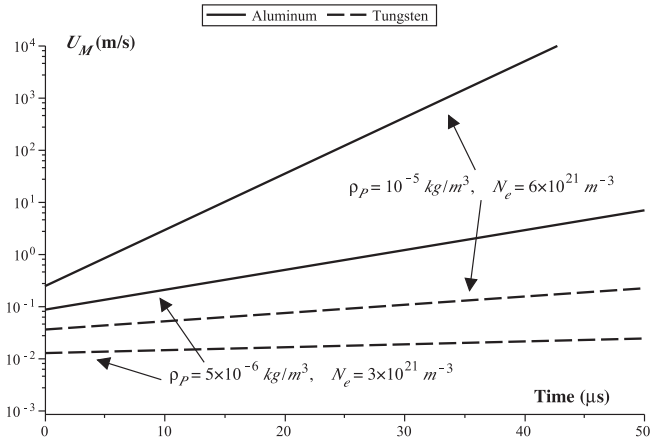

Fig. 6. Instability growth rate for aluminum and tungsten.

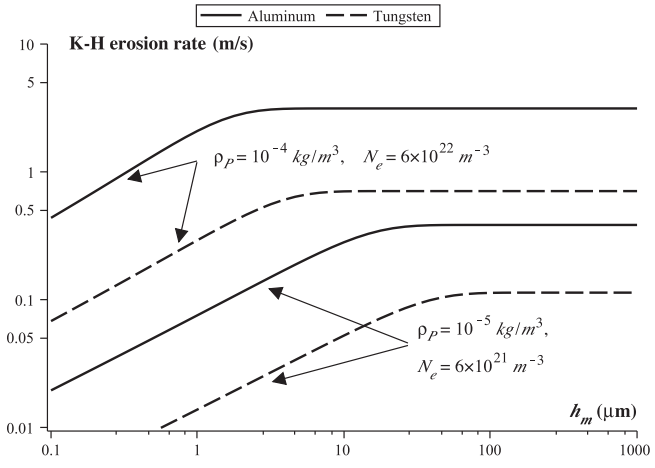

Fig. 7. K–H erosion rate versus melt layer thickness for aluminum and tungsten.

the bulk effect has a lower impact than the surface effect. For relatively high plasma densities, the increment coefficient in Fig. 4 reaches the asymptotic value for a melt layer thickness lower than 100 μm. Using the average value of Eqs. (12) and (13), the most unstable wavelength is 2.2, 0.4, 0.2, and 0.1 mm with increasing values of the plasma density.

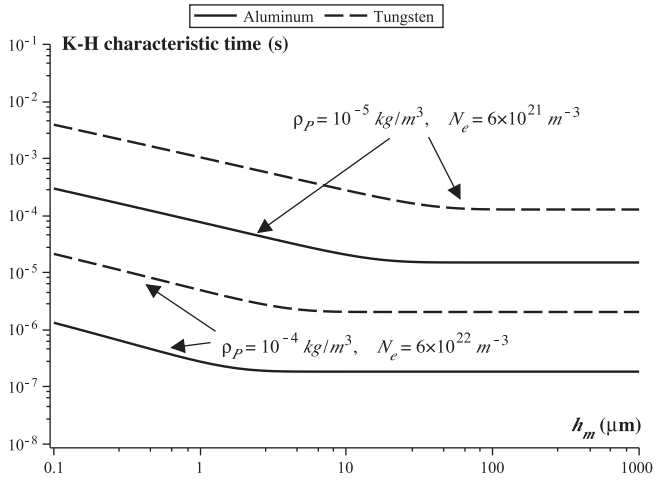

Fig. 8. K–H characteristic time versus melt layer thickness for aluminum and tungsten.

Fig. 5 shows the evolution of the instability growth rate (Eq. (17)) of a 100-micron-thick melt layer, during 50 μs, given that the duration of a typical disruption is 0.1–1 ms. The initial perturbation amplitude ξ_0 usually small compared to the fluid layer thickness, can be originated from several sources. For example, bubbles of ~10 to ~100 μm [7] collapse at the surface of the melt layer due to intense boiling and generate surface waves with amplitudes in the same order of magnitude. To be conservative, the initial perturbation amplitude ξ_0 is chosen equal to 1 μm. According to the growth rate, a plasma stream with a velocity of ~10 km/s and a density lower than $\sim10^{-5}$ kg/m^3 is not expected to cause K–H instabilities on a tungsten target. A more dense plasma, however, could lead to the development of intense K–H instabilities.

Fig. 6 shows the instability growth rate as a function of the time for aluminum and tungsten melts. The effect of different material properties such as surface tension and density on the instability growth rate is illustrated. As expected, the aluminum melt layer with lower density of 2375 kg/m^3 and lower surface tension [20] of 1 N/m becomes very unstable at a relatively low plasma density (5×10^{-6} kg/m^3) while the tungsten melt layer is relatively stable. Besides, under the same heat load, aluminum is expected to have greater melt layer thickness than tungsten, which contributes even more to the growth of the K–H instabilities.

Figs. 7 and 8 show the one-dimensional erosion rate (Eq. (19)) and the characteristic time (Eq. (18)) of droplet ejection due to K–H instabilities, respectively. Two plasma densities (10^{-5} kg/m^3 and 10^{-4} kg/m^3) are used for tungsten and aluminum, which provides two values using Eq. (12) and (13) of the most unstable wavelength for each material. Using the assumption of $r_d = \lambda_M/4$, the sizes of tungsten droplets are respectively 6 and 60 μm. The sizes of aluminum droplets are respectively 2 and 24 μm. Those results are consistent with the observed experimental results [6,7]. At lower plasma density, the erosion rate is negligible for tungsten at small values of the melt layer thickness. Besides, the K–H characteristic time is higher than a typical disruption duration of 0.1 ms for the whole range of melt layer thickness. The erosion rate of aluminum is ~5 times higher than tungsten. At higher density, the erosion of aluminum is about one order of magnitude higher than the erosion of tungsten. The erosion rate is quasi-constant for the range of interest of the melt layer thicknesses (tens to hundreds of microns). Those results do not contradict the theoretical estimation of the erosion rate in [4,5].

With the assumption of a thick melt layer $kh_m \gg 1$, the linear stability analysis provides formula identical to the ones reported

in [5] in terms of the most unstable wavelength and the temporal increment coefficient (Eqs. (13) and (15)). However, using these formula our estimates show that the dense hydrogen plasma with $N \sim 3.5 \times 10^{22}\ m^{-3}$ ($\sim 5.9 \times 10^{-5}\ kg/m^3$) and streaming with $V_p \sim 10^5$ m/s is needed to generate waves on the melt surface with the most unstable wavelength $\lambda_M \sim 40\ \mu m$ in order to produce the droplets with the radius of $\lambda_M/4 \sim 10\ \mu m$. The required density is even larger for the plasma flowing with the lower speed $<10^5$ m/s (Eq. (13)). The parameters of the plasma in the QSPA-T are estimated [5] to be $10^4 < V_p < 10^5$ m/s and $N < 10^{22}\ m^{-3}$. For ITER, the density of the impacting plasma is even lower $10^{19} < N < 10^{20}\ m^{-3}$. In [5], it is assumed that the thickness of a melt layer is larger than the wavelength of the unstable waves and wave breaking does not occur for $kh_m \ll 1$. Such a cut-off condition is not foreseen in our erosion wave model, where the continuous erosion is governed by the erosion rate (Eq. (19)), that is continuously updated according to the characteristic time of droplet ejection. For thinner melt layer, the characteristic time (Fig. 6) increases due to the decrease of the melt layer thickness and thus the erosion rate (Fig. 7) decreases. Therefore, for $kh_m \ll 1$, the erosion due to K–H instabilities still occurs in our model but with a lower velocity.

4. Conclusion

A detailed and comprehensive linear analysis of the K–H instabilities, assuming inviscid and incompressible flows, has been used to study for the first time the macroscopic erosion and splashing of melt layers during intense plasma energy deposition on PFC in tokamak devices. The study shows when the relative velocity between the plasma stream and the liquid layer is below a critical value, which does not depend on the thickness of the melt layer due to the large density difference, no perturbation wave can develop such as K–H instabilities at the interface. However, when the relative velocity is high enough, a range of wavelengths are unstable, among which the most dangerous wave is the fastest one to grow and eventually causes melt layer splashing and erosion. The wavelength of this specific wave depends weakly on the melt layer thickness, whereas the temporal increment of the wave is an increasing function of the thickness at relatively low values and becomes constant at larger values. The growth rate of the most unstable wave is strongly dependent on plasma density and material properties such as surface tension and density. At relatively low plasma density ($10^{-5}\ kg/m^3$), the growth rate of K–H instabilities in tungsten melt layer is negligible and starts being significant in aluminum melt. At higher plasma densities, the capillary effect can induce droplet formation at the surface. The characteristic time of droplets ejection as well as the erosion rate of the melt layer are computed as functions of the instability growth rate. This estimation is justified for short unstable waves with fast growing rate, i.e., for high values of plasma density and low values of surface tension and density of the melt layer.

In the present analysis, the viscous effect is not considered. Viscosity is expected to have a consequent stabilizing effect on the onset of unstable waves. Furthermore, normal components of forces other than gravity could play the role of stabilizing factor. For example, strong magnetic fields of ~5–10 T are present in tokamak devices. When the magnetic field lines, almost parallel to the melt layer surface (~5°), are in the same direction as the plasma flow, a magnetic field induced surface tension is added to the stabilizing factors. However, when the magnetic field lines are transverse to the flow direction, the stability of perturbations is not affected. In the presence of an electric current coupled with the magnetic field, Lorentz force, acting as a body force, could also play an important role in the stability or instability of the perturbations. This work is currently underway.

Acknowledgment

This work is supported by the US Department of Energy, Office of Fusion Energy Sciences.

References

[1] G. Federici, Phys. Scr. T124 (2006) 1.
[2] A. Hassanein, Fusion Technol. 30 (1996) 713–719.
[3] A. Hassanein, V. Belan, et al., J. Nucl. Mater. 241–243 (1997) 288–293.
[4] A. Hassanein, I. Konkashbaev, Suppl. J. Nucl Fusion (1994).
[5] B. Bazylev, G. Janeschitz, I. Landman, et al., Phys. Scr. T128 (2007) 229.
[6] V.N. Litunovsky, V.E. Kuznetsov, et al., Fusion Eng. Des. 49–50 (2000) 249–253.
[7] N.I. Arkhipov, V.P. Bakhtin, et al., Fusion Eng. Des. 49–50 (2000) 151–156.
[8] A. Hassanein, I. Konkashbaev, J. Nucl. Mater. 273 (1999) 326–333.
[9] B. Bazylev, G. Janeschitz, Fusion Eng. Des. 84 (2009) 441–445.
[10] G.V. Miloshevsky, A. Hassanein, Nucl. Fusion 50 (2010) 115005.
[11] G. Miloshevsky, A. Hassanein, Modeling of Macroscopic Melt Layer Splashing during Plasma Instabilities, J. Nucl. Mater., in press, doi: 10.1016/j.jnucmat.2010.08.032.
[12] S. Chandrasekhar, Hydrodynamic and Hydromagnetic Stability, Oxford University, London, 1961.
[13] P.G. Drazin, W.H. Reid, Hydrodynamic Stability, University Press, Cambridge, 1981.
[14] A.B. Brailovsky, Appl. Phys. A 61 (1995) 81–86.
[15] J.W. Coenen et al. Tungsten melt layer motion and splashing on castellated tungsten surfaces at the tokamak TEXTOR, J. Nucl. Mater., in press, doi: 10.1016/j.jnucmat.2010.09.046.
[16] M. Ishii, T. Hibiki, Thermo-fluid Dynamics of Two-Phase Flow, Springer, Purdue University, 2006.
[17] G. Miloshevsky, V. Tolkach, S. Rozin, G. Shani, Nucl. Instrum. Methods Phys. Res. B 168 (2000) 467–472.
[18] V. Tolkach, V. Morozov, A. Hassanein, Development of Comprehensive Models for Opacities and Radiation Transport for IFE Systems, ANL Report, ANL-ET/02-23, July 2002.
[19] J.W. Coenen et al., Analysis of Tungsten Melt Layer Motion and Splashing under Tokamak conditions at TEXTOR, in: Proceedings of 23rd IAEA-FEC Conference, 11–16 October 2010, Daejon, Korea, EXD/6-1.
[20] Kh.Kh. Kalazhokov, Z. Kh. Kalazhokov, Kh. B. Khokonov, Surface Tension of Pure Aluminum Melt, Technical Physics, vol. 48, (2), 2003, pp. 272–273.